

Active Roll Control of Single Unit Heavy Road Vehicles

David J. M. Sampson*

David Cebon†

Cambridge University Engineering Department

Trumpington St, Cambridge CB2 1PZ, UK

Submitted December 2001

Revised October 2002

Submitted to *Vehicle System Dynamics*

*Present address: The MathWorks, Matrix House, Cowley Park, Cambridge CB4 0HH, UK

†Corresponding author, e-mail dc@eng.cam.ac.uk

Summary

Strategies are investigated for controlling active anti-roll systems in single unit heavy road vehicles, so as to maximise roll stability. The achievable roll stability improvements that can be obtained by applying active anti-roll torques to truck suspensions are discussed. Active roll control strategies are developed, based on linear quadratic controllers. It is shown that an effective controller can be designed using the LQG approach, combined with the loop transfer recovery method to ensure adequate stability margins. A roll controller is designed for a torsionally flexible single unit vehicle, and the vehicle response to steady-state and transient cornering manoeuvres is simulated. It is concluded that roll stability can be improved by between 26% and 46% depending on the manoeuvre. Handling stability is also improved significantly.

1 Introduction

1.1 Active roll control for controlling body roll

A passively suspended road vehicle rolls outwards under the influence of lateral acceleration when cornering. Several authors have investigated the use of active roll control to reduce the body roll of heavy vehicles.

Mercedes-Benz developed an active roll control system consisting of switchable air springs (incorporating additional air volume) and switchable dampers for a single unit two axle medium duty truck [17]. The system, which used measurements from driver inputs and other on-board sensors, reduced body roll in lane change manoeuvres by 30-50%.

Kusahara et al. also investigated the use of an active roll control system to reduce the body roll of a single unit truck [9]. The active roll control system consisted of anti-roll bars front and rear linked to the vehicle frame by single rod double-acting hydraulic actuators. By extending or contracting the hydraulic actuators, the vehicle body roll angle could be controlled. Wheel speed and steering angle sensors were used to estimate the lateral acceleration of the vehicle, which was input to a proportional feedforward controller to produce actuator force demand signals. The controller could switch between several modes for different loading conditions by measuring the static suspension deflections when the vehicle was at rest. The system reduced body roll by 67% in steady-state cornering and in high speed lane changes. The authors attributed some differences between predicted and measured responses to excessive torsional flexibility of the vehicle frame. The active roll control system could be deactivated during straight running to improve ride performance. Used in conjunction with an active rear wheel steering system, the active roll control system provided a small improvement in directional controllability. Subjective tests showed that the system improved overall driver comfort.

1.2 Active roll control for enhancing roll stability

Recently the use of active roll control systems to improve vehicle roll stability and reduce the likelihood of roll-over accidents has been proposed by several authors [4, 12, 13, 15]. The centre of sprung mass of passively suspended vehicles shifts outboard of the vehicle centreline during cornering. This contributes a destabilising moment that reduces roll stability. (See [19] for a complete analysis.) The aim of a stabilising active roll control system is to lean the vehicle *into* corners such that the centre of sprung mass shifts inboard of the vehicle centreline and contributes a stabilising roll moment.

Lin et al. investigated the use of an active roll control system to reduce the total lateral load transfer response of a single unit truck to steering inputs [12, 13, 15]. A linear model with four degrees of freedom (yaw, sideslip, sprung mass roll angle and unsprung mass roll angle) was used. A steering input spectrum was derived by considering the low frequency steering inputs required to follow the road (based on road alignment data) as well as the higher frequency inputs needed to perform frequent lane change manoeuvres. Combining the spectral densities from these low and high frequency sources, they found that, for a very active level of driver input on a typical road, the steering input spectrum could be modelled approximately by white noise filtered by a low pass filter with a cut-off frequency of 4 rad/s [12]. This spectrum was used by Lin et al. to design an optimal full state linear quadratic controller to regulate load transfer. This control scheme caused the vehicle to lean into corners. The lateral acceleration level at which wheel lift-off is first achieved was increased by 66% and the total RMS load transfers in response to a random steering input were reduced by 34%. A proportional-derivative lateral acceleration feedback controller was also designed using pole placement. Although the reductions in total load transfer were smaller, the lateral acceleration controller was attractive because of its simpler instrumentation requirements. The effects of actuation system bandwidth were also considered. A bandwidth of 3 Hz was found to give satisfactory performance, and increasing bandwidth above 6 Hz gave no improvement in performance. The average

power requirement was 17 kW for a “worst case” steering input.

1.3 Active roll moment distribution

Directional stability and handling performance are strongly influenced by the distribution of roll stiffness among the axles of a vehicle because of the nonlinear relationship between normal tyre load and cornering stiffness, particularly for truck tyres. In the absence of torsional frame flexibility, axles with greater roll stiffness will carry a greater proportion of the total lateral load transfer generated during cornering. This leads to an effective reduction of cornering stiffness at those axles, affecting the handling balance [6, 22]. Several authors have investigated the possibility of influencing automobile handling through using advanced suspensions to vary roll moment distribution [1, 7, 24]. These studies showed that, using active control of roll moment distribution, it is possible to improve vehicle handling response and stability.

2 Vehicle modelling

In this study, linearised models of the roll and handling dynamics of heavy vehicles were used for active roll control system design. Vehicle models including nonlinear tyre behaviour were used to simulate handling performance.

2.1 Linear single unit vehicle model

The linear model used to describe the roll and handling response of a single unit vehicle to steering inputs, built on models formulated by Segel [21] and Lin [12]. Pitching and bouncing motions have only a small effect on the roll and handling behaviour of the vehicle and so were neglected in formulating a yaw-roll model. The effects of aerodynamic inputs (wind disturbances) and road inputs (cross-gradients, dips and bumps) were also neglected.

The single unit vehicle (figure 1) was modelled using four bodies – two to represent the sprung mass, and one each for the front and rear axles. Multiple axles at the front or rear of a vehicle unit were simulated by lumping their effects into a single equivalent axle group.

The vehicle as a whole had freedom to translate longitudinally and laterally, and could yaw. The sprung mass could rotate about a horizontal axis (the *roll axis*) fixed in the unsprung masses. The location of the roll axis is dependent on the kinematic properties of the front and rear suspensions. The unsprung masses could also rotate in roll relative to the sprung mass, enabling the effect of the vertical compliance of the tyres on the roll performance to be included in the model.

The equations of motion of the vehicle were formulated by equating the rates of change of momentum (or, in the rotational case, moment of momentum) with the sum of external forces (or moments) acting on the system. The motion was described using a coordinate system (x', y', z') fixed in the vehicle (figure 1). The roll axis was replaced by an x' axis parallel to the ground, and the z' axis passed downward through the centre of mass of the vehicle.

The suspension springs, dampers and anti-roll bars generate moments between the sprung and unsprung masses in response to roll motions. The active roll control systems at each axle consisted of a pair of actuators and mechanical linkages in parallel with the existing passive springs and dampers. This active roll control system generated additional (controlled) roll moments between the sprung and unsprung masses.

The tyres produce lateral forces that vary linearly with slip angle. This assumption of linearity is reasonable for lateral motions of moderate amplitude. The effects of aligning moment, camber thrust, roll steer and rolling resistance generated by the tyres are of secondary importance and were neglected.

The linear model assumed that the forward speed of the vehicle is constant during any lateral manoeuvre. (Although forward speed is an important stability parameter, it was not considered to be a variable of motion.) The driving thrust remained constant and was evenly distributed between the driving wheels, so did not contribute a yaw moment about the centre of mass. The driving thrust and lateral load transfer were assumed not to affect the lateral mechanical properties of the tyres in the linear case.

The roll stiffness and damping of the vehicle suspension systems were assumed to be constant for the range of roll motions considered.

The nonlinear effects of varying speed and tyre and suspension properties on the stability and performance of the system were considered separately.

Previous investigations into the use of active roll control systems on heavy vehicles have all used the assumption that the vehicle frame is a rigid body. However, torsional compliance of the vehicle frame influences the distribution of roll moments between axle groups, and significant frame compliance might be expected to affect roll and handling performance noticeably. Winkler et al. noted that “the torsional compliance of the vehicle frame stands out as a uniquely important element in establishing the roll stability of some vehicles, particularly those with flat-bed trailers” [25]. It is essential to include the torsional flexibility of the frame in the vehicle model to predict the roll-over threshold of such vehicles accurately.

In order to represent the torsional flexibility of a vehicle frame, it is necessary either

to model the frame as a series of two or more rigid bodies (interconnected by joints of appropriate torsional stiffness), or to embed a complex model of the frame within the existing rigid body formulation.

Since the motivation for including the frame flexibility was only to capture the influence of compliance on the distribution of roll moments between axles, a simple model of the frame using two rigid bodies was sufficient. The sprung mass was split into front and rear sections, each with appropriate inertial properties, as shown in figure 1. These two sections of the sprung mass were connected with a torsional spring whose stiffness matched the torsional stiffness of the vehicle frame. The torsional spring was sited at the centroid height of the frame, so that the line of action of the lateral shear force in the vehicle frame was properly represented. A small amount of torsional damping, representing the energy dissipation inherent in the structure of the vehicle frame, is also included.

The equations of motion for the linear torsionally flexible single unit vehicle model are given in appendix A. Model parameter values are provided in appendix B. Nomenclature is detailed in appendix C.

2.2 Nonlinear extensions to linear models

Simplified models of the nonlinear characteristics of tyres and suspensions, sufficient for analysing the effect of nonlinearities on roll stability and vehicle handling, are presented below.

2.2.1 Nonlinear tyre behaviour

The nonlinear variation of tyre cornering stiffness F_y/α with vertical load F_z is described using the quadratic equation

$$\frac{F_y}{\alpha} = c_1 \times F_z + c_2 \times F_z^2 \quad (1)$$

where c_1 and c_2 are constants. This equation is generally suitable for lateral accelerations up to the roll-over point and is widely used in heavy vehicle simulation studies [5].

2.2.2 Nonlinear suspension behaviour

The dominant nonlinear feature of the suspension behaviour occurs when the suspension roll angle reaches the maximum allowable angle. At this point the axles come into contact with the solid rubber bump stops, causing the roll stiffness to increase dramatically.

The springs and dampers also exhibit certain nonlinear force-deflection and force-velocity behaviours respectively. These behaviours are highly component-specific and were modelled using fitted data provided by the manufacturers. The geometric non-linearity between wheel deflection and spring or damper deflection is a function of the kinematics of the suspension linkages. It is important to note, however, that the effects of component and geometric nonlinearities on roll stiffness and roll damping in percentage terms are typically small, particularly for air suspensions.

2.3 Active roll control system model

The active roll control system at an axle group generates a roll moment between the sprung and unsprung masses in response to a demand signal from the controller. The control torques u_f and u_r acting between the axle groups and the sprung mass are shown in figure 1.

A detailed model of all mechanical and hydraulic components of the active roll control system is necessary for designing a roll moment local controller. However a reduced order model of the transfer function, from torque demanded to torque delivered, is appropriate for designing the global controller. The dynamics of the actuators, the maximum flow rate through the servo-valves and the roll-plane dynamics of the vehicle all influence the achievable system bandwidth.

McKevitt [16] performed detailed design studies of suitable active anti-roll bar hardware and of the local controller algorithms required to control this hardware. He reported that the closed-loop transfer function of a suitable system could be approximated using a first order lag. While this parametrisation is clearly dependent on the design of the active roll control system, a detailed investigation of the achievable dynamics of such systems is outside the scope of the present study.

3 Achievable roll stability

Roll stability is best quantified by the roll-over threshold, which is the limit of steady-state lateral acceleration that a vehicle can sustain without rolling over. Roll-over occurs when the vehicle is unable to provide a stabilising net restoring moment in response to an overturning moment. Since the roll motions at the front and rear of a single unit vehicle unit are coupled, wheel lift-off at a particular axle does not necessarily imply a loss of roll stability of the entire vehicle. A stability analysis can be used to identify the critical axle lift-off that defines the roll-over threshold.

It is shown by a controllability analysis detailed in [19, 20], that it is not possible to control all axle load transfers and body roll angles independently using active anti-roll bars alone. Consequently it is generally not possible to simultaneously maximise both the restoring moment at each axle (by using the full lateral load transfer capacity) and the stabilising lateral displacement moment (by tilting all vehicle units into a turn at the maximum angle). Roll stability of a vehicle with an ideal active roll control system is ultimately limited by the available suspension travel.

There is an apparent compromise between the aims of maximising the restoring moment provided by the axles and maximising the stabilising lateral displacement provided by the inward tilt of the vehicle units. However it turns out that these control objectives yield identical roll-over thresholds (see details in [19, 20]). It is found that the best control strategy is to set the normalised load transfers at all critical axles to be equal while taking the maximum inward roll angle among the sprung masses to the maximum angle allowed by the suspension travel.

4 Active roll control of a single unit vehicle

In this section, an active roll control system is designed for a single unit heavy vehicle, based on the results of the controllability analysis described in the previous section.

4.1 Vehicle description

The single unit vehicle is a two axle tractor unit, as would typically be used to tow a tanker semi-trailer. The vehicle parameters are from an experimental tractor unit, fitted with an active roll control system, that is currently being designed and built by members of the Cambridge Vehicle Dynamics Consortium in the UK. The unit has a wheelbase of 3.7 m, with a pair of single tyres on the steer axle and a pair of twin tyres on the drive axle. The unladen axle weights are 4559 kg on the steer axle and 1966 kg on the drive axle. The torsional stiffness of the vehicle frame is estimated at 629 kN.m/rad. The complete set of vehicle parameters is given in appendix B.

A lumped mass of 8828 kg is attached above the fifth wheel, with the centre of this mass at a height of 2.475 m above ground. This mass was chosen to represent the portion of a fully laden tanker semi-trailer that is supported by the tractor unit at the fifth wheel coupling. The height was selected to give the same body roll angle as the tractor semi-trailer for a given level of lateral acceleration. This approach has been used in previous studies [12, 15] and serves as a starting point from which to build up to a study of tractor semi-trailers and longer combination vehicles. While the single unit vehicle model is less complex than the tractor semi-trailer that it approximates, the response characteristics (for example, the actuator forces and servo-valve flow rates) are comparable.

4.1.1 Control system hardware

The active roll control system at an axle group generates a roll moment between the sprung and unsprung masses in response to a demand signal from the controller. The system is based on a conventional trailing arm suspension and is illustrated in figure 3.

Air springs between the trailing arms and the vehicle frame provide ride suspension and passive roll stiffness. A stiff U-shaped anti-roll bar is connected to the trailing arms directly and to the vehicle frame by a pair of double-acting hydraulic actuators. The position of the anti-roll bar is therefore determined by both the wheel positions and the actuator positions. By extending one actuator and retracting the other, it is possible to apply a roll moment to the sprung mass and tilt the vehicle body.

4.2 Control system design objectives

A torsionally flexible single unit vehicle has four roll outputs (the body roll angles at the front and rear of the vehicle and the load transfers at the steer and drive axles) and two roll control inputs. The system is therefore *input deficient* [19]. Without active roll control, the system is stable (with poles at $-1.58 \pm j3.39$, $-14.1 \pm j5.50$, $-3.78 \pm j20.8$, -583 and -602 rad/s) and minimum phase. The eigenvalue analysis shows that, for a frame stiffness of 629 kN.m/rad, it is still possible for the vehicle (both with and without active roll control) to maintain roll stability after either the steer or drive axle lifts off, so it is important to control the load transfers at both axles. By the results presented in section 3, the achievable design objective that maximises the roll stability of the vehicle is to set the normalised load transfers at the steer and drive axles to be equal while taking the larger suspension roll angle to the maximum allowable inward angle.

4.3 \mathcal{H}_2 control techniques

4.3.1 Linear quadratic regulator problem

The standard LQR problem is to find the control $u(t)$ that minimises the quadratic performance index

$$J = \int_0^{\infty} (z^T Q z + u^T R u) dt \quad (2)$$

for a strictly proper system

$$\dot{x} = Ax + B_0u, \quad z = C_1x, \quad (3)$$

where the matrices Q and R are design parameters representing the relative weighting of the performance output trajectory z and the control input u respectively.

The optimal control law [2] is provided by a state feedback controller

$$u(t) = K_{FB}x(t) \quad (4)$$

where

$$K_{FB} = -R^{-1}B_0^T S \quad (5)$$

and where S is a symmetric, positive semidefinite matrix satisfying the Riccati equation

$$SA^T + A^T S - SB_0R^{-1}B_0^T S + C_1^T Q C_1 = 0. \quad (6)$$

The resulting closed loop feedback system is asymptotically stable.

4.3.2 Linear quadratic regulator with constant disturbance

The standard LQR approach is used to synthesise an optimal controller for the special case of zero input disturbance, as described by equation (3). However the problem of vehicle roll control is a problem of optimal disturbance rejection. The aim is to regulate load transfers in response to steering inputs from the driver.

It can be shown that the optimal control law for a system with a constant input disturbance consists of the solution to the standard LQR problem (equation (4)) plus a feedforward controller operating on the input disturbance [11, 19].

4.3.3 Optimal disturbance rejection system design

Vehicles are subjected to a range of different transient steering inputs which may all be equally likely. It is important to design a controller that is optimised over this range of disturbances rather than for one particular transient input (for example steady state cornering or a specific lane change manoeuvre [12, 15]).

Effective disturbance rejection can be achieved if the dynamic properties of the disturbance are modelled and included in the controller design [11]. *For optimal disturbance rejection, the disturbance inputs must be measured or estimated such that the feedback of the disturbance states to the controller becomes part of the feedback law [11].*

The steering input to a vehicle can be modelled as a zero-mean coloured stochastic process [12, 15]. This can be described by a shaping filter (A_D, B_D, C_D, D_D) such that a zero-mean white noise source w at the input to the filter produces an appropriately time correlated stochastic steering disturbance δ at the output:

$$\dot{x}_D = A_D x_D + B_D w, \quad \delta = C_D x_D + D_D w. \quad (7)$$

Note that the shaping filter required to describe typical steering inputs is in the form of a low-pass filter (with $D_D = 0$), of first order [12, 14]. This form is convenient since the disturbance states x_D can be reconstructed from the filter output δ without knowledge of the white noise input w .

The steering disturbance δ from equation (14) then acts as the input to the vehicle system through the input injection node described by the matrix B_1 such that the dynamics of the system are described by

$$\begin{aligned} \dot{x} &= Ax + B_0 u + B_1 \delta \\ &= Ax + B_0 u + B_1 C_D x_D + B_1 D_D w, \end{aligned} \quad (8)$$

as shown in figure 4(a).

Equation (8) can be rewritten by forming an augmented state vector \underline{x} including the system states x and the disturbance state x_D such that the dynamics of the system are described by

$$\dot{\underline{x}} = \underline{A}\underline{x} + \underline{B}_0u + \underline{B}_1w \quad (9)$$

where

$$\underline{x} = \begin{bmatrix} x \\ x_D \end{bmatrix}, \quad \underline{A} = \begin{bmatrix} A & B_1C_D \\ 0 & A_D \end{bmatrix}, \quad \underline{B}_0 = \begin{bmatrix} B_0 \\ 0 \end{bmatrix}, \quad \underline{B}_1 = \begin{bmatrix} B_1D_D \\ B_D \end{bmatrix}.$$

Since x_D is a disturbance state, the optimal control is chosen to minimise the performance index described in equation (2). The optimal controller is a feedback controller K_{FB} operating on \underline{x} , and the optimal control law is given by

$$u(t) = K_{FB}\underline{x}(t) \quad (10)$$

where

$$K_{FB} = -R^{-1}\underline{B}_0^T S \quad (11)$$

and where S is the solution to the appropriate Riccati equation. The controller configuration is shown in figure 4(b).

Partitioning the feedback controller $K_{FB} = \begin{bmatrix} K_{FB,1} & K_{FB,2} \end{bmatrix}$ such that $K_{FB,1}$ denotes the gain on x and $K_{FB,2}$ denotes the gain on x_D , the closed loop system is described by

$$\begin{bmatrix} \dot{x} \\ \dot{x}_D \end{bmatrix} = \begin{bmatrix} A + B_0K_{FB,1} & B_1C_D + B_0K_{FB,2} \\ 0 & A_D \end{bmatrix} \begin{bmatrix} x \\ x_D \end{bmatrix} + \begin{bmatrix} B_1D_D \\ B_D \end{bmatrix} w. \quad (12)$$

The term $B_0K_{FB,2}$ acts as a feedforward control on the disturbance states x_D . This feedforward action reduces the response of the closed loop system to stochastic disturbances. However the stability of the closed loop system is unaffected by this feedforward control since the closed loop eigenvalues of the system are simply the eigenvalues

of $A + B_0 K_{FB,1}$ and A_D . By contrast, for the case where x_D is estimated from the system response rather than measured, $K_{FB,2}$ becomes part of the feedback loop and therefore can affect the stability.

4.3.4 Robustness properties of LQR control

An LQR-controlled system with no stochastic process noise or measurement noise has favourable guaranteed stability margins: a gain margin of infinity, a gain reduction margin of 0.5, and a phase margin of at least 60° at each control input [8, 18]. (A necessary condition is that the weight R is chosen to be diagonal.)

4.3.5 Linear quadratic Gaussian problem

It is not practical to measure all internal states of the system. Furthermore the sensor output signals will be corrupted to some extent by noise, so to deduce the states accurately even from a complete set of measured outputs is not straightforward.

A more realistic system model is

$$\dot{\underline{x}} = \underline{A}\underline{x} + \underline{B}_0 u + \underline{B}_1 w, \quad \underline{y} = \underline{C}_0 \underline{x} + v, \quad (13)$$

where w and v are vectors representing the process noise and measurement noise respectively. The process noise w in this case is due to steering inputs from the driver. The measurement noise v is due to sensor inaccuracies and electrical interference. It is possible to incorporate coloured noise inputs into the LQG framework by augmenting the vehicle system model with shaping filters at the disturbance inputs.

By the *separation principle*, the solution to the LQG problem consists of an optimal state estimator and an optimal state feedback controller that are designed independently [10]. The optimal state feedback controller is a linear quadratic regulator as described in section 4.3.3. The optimal state estimator under additive process and measurement noise is a Kalman filter [23].

4.3.6 Robustness properties of LQG control

It is important to note that Kalman filter design must be carried out carefully to ensure that the resulting LQG controller has similar robustness properties and transient performance as the full-state LQR design. This may be achieved using the *loop transfer recovery* (LTR) method, which is a technique for indirectly shaping the singular values of the LQG loop transfer function with the aim of recovering the favourable guaranteed stability margins of LQR control [3].

The two step LQG-LTR control design procedure consists of a *loopshaping* step and a *recovery* step. In the loopshaping step, the regulator design parameters Q and R are varied to design a full-state linear quadratic regulator with favourable time domain and frequency domain characteristics. The LQR loop transfer function then becomes the *target feedback loop* transfer function. In the recovery step, the filter design parameters W and V , which represent the relative weighting of the process noise and measurement noise respectively, are varied until the full LQG loop transfer function is acceptably close to the target feedback loop transfer function. As $V \rightarrow 0$ (or equivalently as $W \rightarrow \infty$), the LQG loop transfer function will asymptotically approach the target feedback loop transfer function.

4.4 Control of a torsionally flexible single unit vehicle

4.4.1 Design of a full-state feedback controller

As mentioned in section 1.2, Lin estimated that a typical steering input spectrum could be modelled by white noise filtered by a low pass filter with a cut-off frequency of 4 rad/s [12]:

$$\dot{x}_D = -4x_D + 2w, \quad \delta = 2x_D. \quad (14)$$

Optimal control in this case requires that the control law minimises the performance index in equation (2). The weighting matrices Q and R (equation (2)) penalise the performance output z and the control input u respectively. In order to simplify the

selection of these matrices, the elements of Q are chosen to penalise only the unsprung mass roll angle terms (since the load transfer at an axle is equal to the unsprung mass roll angle multiplied by the effective roll stiffness of the tyres), hence

$$z = \begin{bmatrix} \phi_{t,f} & \phi_{t,r} \end{bmatrix}^T. \quad (15)$$

The constraint on suspension roll angles is handled implicitly by selecting the elements of R to be sufficiently large to limit the roll moments from the active anti-roll bars, since excessive roll moments lead to excessive inward roll angles. A useful starting point for selecting the elements of the weighting matrices is to choose Q and R as diagonal matrices

$$Q = \begin{bmatrix} q_1 & 0 \\ 0 & q_2 \end{bmatrix}, \quad q_i = (z_{i,\max})^{-2} \quad (16)$$

and

$$R = \begin{bmatrix} r_1 & 0 \\ 0 & r_2 \end{bmatrix}, \quad r_i = (u_{i,\max})^{-2} \quad (17)$$

where $z_{i,\max}$ and $u_{i,\max}$ are respectively the maximum acceptable values of the i th elements of the performance output vector and control input vector [2]. From this starting point, an iterative design process follows in which the elements of Q and R are tuned to produce a controller with acceptable performance across a range of manoeuvres. The following tuning procedure can be used for a range of vehicles, and was found to produce good performance with a reasonably limited number of design iterations [19]:

1. Adjust the elements of Q and R to tune the steady-state performance of the system such that the normalised load transfers at all critical axles* are balanced and the maximum inward suspension roll angle at any axle at roll-over is around 4° . (The maximum suspension roll angle allowed is typically $6-7^\circ$.) Although

*Since the roll motions of the axles are coupled, wheel lift-off at a particular axle does not necessarily imply a loss of roll stability for the entire vehicle. A stability analysis [19, 20] can be used to identify the *critical* axles, the lift-off of which governs the roll-over threshold.

this may seem conservative, the largest steady-state suspension roll angle should be less than the maximum allowable angle to leave space for overshoot in severe transient manoeuvres; otherwise the axles will strike the bump stops.

2. Simulate the performance of the vehicle for a range of severe transient manoeuvres including step steering inputs and lane changes.
3. If the maximum transient suspension roll angle in response to any critical[†] transient manoeuvre is greater than the maximum allowable angle, then the step 1 should be repeated with the largest steady-state inward suspension roll angle at roll-over reduced.
4. If the peak normalised load transfer responses among the axles are poorly balanced in severe transient manoeuvres, it is necessary to adjust the elements of Q and R . This will necessarily require a compromise in the steady-state moment balance. The compromise required is typically larger for more torsionally flexible single unit vehicles and for articulated vehicles. This is particularly the case when a high level of rearward amplification is present, for example at high speed or where pintle hitch couplings are used.

For a speed of 60 km/h, the weighting matrices were chosen to be

$$Q = \begin{bmatrix} 1.00 & 0 \\ 0 & 2.08 \end{bmatrix} \text{rad}^{-2}, \quad (18)$$

$$R = 3.35 \times 10^{-14} \begin{bmatrix} 1 & 0 \\ 0 & 1 \end{bmatrix} \text{N}^{-2} \cdot \text{m}^{-2}. \quad (19)$$

This produced a full-state feedback controller detailed in [19]. The performance of this controller is examined in detail in the following sections.

[†]A manoeuvre is described as *critical* when the size of the steering input is just sufficient to induce roll-over.

4.4.2 Steady-state cornering response

The response of the linear, torsionally flexible single unit vehicle model to a steady-state steering input at 60 km/h is shown in figure 5.

Without active roll control (that is, passive suspension), the vehicle rolls out of the corner (negative roll angle). The normalised load transfer builds up more quickly at the drive axle than at the steer axle, and this effect becomes more pronounced as torsional flexibility of the frame increases. The inner drive axle tyre lifts off the ground at 0.38 g (point *A*), at which point the normalised load transfer at the steer axle is 0.67 (point *B*). As lateral acceleration increases, the slopes of the suspension roll angle and normalised load transfer curves increase, and the normalised load transfer at the steer axle reaches the critical value of 1 at 0.40 g (point *C*).

With active roll control, the vehicle rolls into the corner. The total roll moment is distributed between the active anti-roll bars so that the normalised load transfers at the two axles increase in a balanced fashion as lateral acceleration increases. This requires a relative twist angle between the front and rear sections of the vehicle of $5.7^\circ/\text{g}$, with the front section rolling into the corner more than the rear. For a more torsionally flexible vehicle frame, the twist angle required to balance the normalised load transfers is greater. The normalised load transfers at both axles reach the critical value of 1 at 0.51 g (point *D*), at which point the steer axle suspension roll angle is 3.4° inward. This represents a 5% reduction in roll-over threshold compared to a vehicle with a torsionally rigid frame but with all other parameters unchanged [19].

Active roll control increases the roll-over threshold of the torsionally flexible single unit vehicle by 26% compared with the passive case and the lateral acceleration at which axle lift-off first occurs by 33%. This is a substantial improvement in steady-state roll stability. The benefits are derived from: (1) balancing the roll moments so that the steer axle carries its fair share of the total roll moment; and, (2) tilting the vehicle towards the centre of the turn.

A parametric study in [19] suggests that the achievable improvements to roll stability offered by active roll control systems are greater for torsionally flexible vehicles

than for torsionally rigid vehicles.

4.4.3 Response to a step steering input

The response of the linear, torsionally flexible single unit vehicle model to a step steering input is shown in figure 6. The step input is scaled to give a maximum normalised load transfer of 1 in the following simulations.

The lateral acceleration response is shown in figure 6(a). The steady-state lateral acceleration is 0.34 g. The active roll control system eliminates the small lateral acceleration overshoot that is present in the passive response.

The suspension roll angle responses are shown in figure 6(b). Without active roll control, the vehicle rolls out of the corner (negative roll angle) by 3.2° and 4.3° at the steer and drive axles respectively. There is a small overshoot in both traces. The roll angle at the drive axle exceeds that at the steer axle because the majority of the vehicle mass is high at the rear and so the moment of the inertial force due to cornering there is very large. With active roll control, the vehicle rolls into the corner by 2.3° at the steer axle and 0.2° at the drive axle, with peak values of 3.0° and 1.4° respectively. While the overshoot of the steer axle suspension roll angle response is undesirable, a reduction in overshoot would lead to an increase in load transfer. The difference between the front and rear roll angles is generated in order to twist the frame so as to transfer some overturning moment from the rear to the front. This balances the normalised load transfers and minimising the performance index described in equation (2).

The normalised load transfer responses are shown in figure 6(c). Without active roll control, the normalised load transfer builds up more quickly at the drive axle than at the steer axle. This trend is more apparent for more flexible vehicle frames. That is, frame flexibility reduces the ability of the steer axle to carry its share of the total lateral load transfer. The normalised load transfer responses feature moderate overshoots before settling at final values of 0.60 and 0.91 for the steer and drive axles respectively. In addition to reducing the total lateral load transfer by rolling the vehicle into the turn, the active roll control system redistributes the load transfer in a balanced fashion between

the axles so that both show a peak normalised value of 0.68. The system reduces the peak load transfer at the drive axle by 32%. The load transfer at the steer axle increases, although this is because, in the passive case, the steer axle carries much less than its fair share of the total load transfer.

The results in section 4.4.2 (figure 5) show that the roll-over threshold of the vehicle with passive suspension is just 6% higher than the level of lateral acceleration at which the drive axle lifts off. By contrast, the active roll control system can retain roll stability with up to 46% additional lateral acceleration (that is, up to 0.51 g). This represents a significant enhancement in roll stability.

Figure 6(d) shows that, for the torsionally flexible vehicle, 46% of the total active roll moment is generated at the drive axle. (For a torsionally rigid vehicle with active roll control, 59% of the total roll moment is generated at the drive axle.) The peak roll moment in response to a critical steering input is 63 kN.m at the steer axle.

The hydraulic fluid flow rates are shown in figure 6(e). By scaling up the responses, it is possible to predict the peak fluid flow rate and the peak power supplied to the system in a critical manoeuvre. The peak flow rates in response to a critical step input were found to be 1.17 l/s at the steer axle and 0.62 l/s at the drive axle, and the peak power supplied was 5.9 kW (neglecting losses) [19].

4.4.4 Response to a double lane change steering input

The response of the linear, torsionally flexible single unit vehicle model to a double lane change steering input at 60 km/h is illustrated in figure 7. (See [19] for more details of the manoeuvre.) The path deviation in this manoeuvre was 5 m over a 120 m test section, with a peak lateral acceleration of just under 0.2 g (see figure 7(a)).

The suspension roll angle responses are shown in figure 7(b). The patterns from sections 4.4.2 and 4.4.3 are again evident. The vehicle without active roll control rolls out of the corner while the vehicle with active roll control rolls into the corner. There is a relative roll angle between the front and rear sections of the vehicle both with and without the active roll control system, with the front section always rolling more

towards the inside of the corner.

The normalised load transfer responses are shown in figure 7(c). The active roll control system balances the normalised load transfers between the axles effectively, reducing the peak normalised drive axle load transfer by 43% (from 0.68 to 0.39) with little change in the peak normalised steer axle load transfer. That is, the vehicle with active roll control could remain stable even if the steering input was scaled up by 157%. This represents a greater relative improvement in roll stability than was achieved for a torsionally rigid vehicle of similar specification, although the ultimate roll stability of the rigid vehicle is higher [19].

It should be noted that the double lane change manoeuvre generates larger suspension roll angles per normalised load transfer than the steady-state or step manoeuvres. The peak inward roll angle at the steer axle in response to a critical steering input is 6.2° , which is around the limit of the available travel for typical heavy vehicle suspensions.

Figure 7(d) shows that the peak active anti-roll bar moments at the steer and drive axles are of comparable magnitude, with the roll moment at the drive axle slightly higher. The peak roll moment in response to a critical double lane change steering input is 82 kN.m

The servo-valve flow rate responses are shown in figure 7(e). The peak flow rates in response to a critical double lane change manoeuvre were found to be 1.82 l/s and 1.18 l/s at the steer axle and drive axle respectively. When compared with the peak flow rates for the torsionally rigid vehicle, the required servo-valve capacity is similar at the steer axle and is significantly lower at the drive axle because the roll angle and roll rate responses are reduced. The forced oscillation frequency of the vehicle body in roll is dictated by the steering input and the maximum roll angle is set by the suspension travel. This means that the axles with the largest amplitude of suspension roll should be expected on average to have the highest roll rates and therefore the highest fluid flow rates. The peak power supplied to the system in response to a critical step input is 14.7 kW (neglecting losses).

4.4.5 Design of a partial-state feedback controller

A partial-state feedback controller was designed using the LQG-LTR procedure. The controller used measurements of the suspension roll angles at both the steer and drive axles, plus the body roll rate at the rear, the yaw rate and the steering input,

$$y = \begin{bmatrix} \phi_f - \phi_{t,f} & \phi_r - \phi_{t,r} & \dot{\phi}_r & \dot{\psi} & \delta/2 \end{bmatrix}^T. \quad (20)$$

The unmeasured vehicle states were the body roll rate at the front, the sideslip angle and the lateral load transfers at both axles.

For the Kalman filter design, the elements of the measurement noise weighting matrix W were chosen to be

$$W = \begin{bmatrix} 1.00 & 0 & 0 & 0 & 0 \\ 0 & 1.00 & 0 & 0 & 0 \\ 0 & 0 & 1.00 & 0 & 0 \\ 0 & 0 & 0 & 0.50 & 0 \\ 0 & 0 & 0 & 0 & 1.29 \end{bmatrix}^T \begin{matrix} \text{rad}^{-2} \\ \text{rad}^{-2} \\ \text{rad}^{-2} \cdot \text{s}^2 \\ \text{rad}^{-2} \cdot \text{s}^2 \\ \text{rad}^{-2} \end{matrix} \quad (21)$$

and the process noise weighting V was varied as a tuning parameter from 1 rad^{-2} down to 0.001 rad^{-2} . The target feedback loop is that of the full-state feedback controller described in section 4.4.2.

The frequency responses of the steer axle suspension roll angle, steer axle load transfer and drive axle load transfer to a steering input are shown as a function of V in figure 8. (The results are similar to those presented for the torsionally rigid single unit vehicle in [19].) For $V = 1 \text{ rad}^{-2}$ and $V = 0.1 \text{ rad}^{-2}$, there are significant differences from the target (full-state feedback) response in the magnitude of the suspension roll angles at low frequency and in the phase of the drive axle load transfer above 4 rad/s . As V is reduced, the frequency responses converge towards the target response.

The transient performances of several LQG-controlled designs to a step steering input are compared in figure 9. Random, uncorrelated white measurement noise of 5%

RMS on each measurement channel has been added to each measurement channel. The load transfer performance of the system improves as V is reduced from 1 rad^{-2} , and by $V = 0.001 \text{ rad}^{-2}$ there is little difference in the performance of the LQR-controlled and LQG-controlled systems. The random measurement noise is effectively attenuated. It is apparent that the improvements to roll stability offered by a full-state feedback controller are also available using a partial-state feedback controller.

4.4.6 Effect of actuator performance limitations

Figure 10 illustrates the effect of the limited bandwidth of the active roll control system on the response of the linear, torsionally flexible single unit vehicle model with a full-state feedback (LQR) controller to a step steering input. The active roll control system was represented with a 0.5 Hz first order low-pass filter and a new controller was synthesised to give the same steady-state performance as in section 4.4.2. The new Q and R matrices were

$$Q = \begin{bmatrix} 1.00 & 0 \\ 0 & 1.85 \end{bmatrix} \text{rad}^{-2}, \quad (22)$$

$$R = 1.18 \times 10^{-14} \begin{bmatrix} 1 & 0 \\ 0 & 1 \end{bmatrix} \text{N}^{-2} \cdot \text{m}^{-2}. \quad (23)$$

Limiting the bandwidth of the active roll control system increases the rise time of the roll angle responses (see figure 10(a)). For this particular manoeuvre, however, the increases in peak normalised load transfers at both axles are negligible, as illustrated in figures 10(b) and 10(c). The peak flow rates through the servo-valves are reduced by 8% and 23% at the steer and drive axles respectively, as shown in figure 10(e).

4.4.7 Stability robustness to vehicle parameter uncertainty

The properties of vehicle components vary with different operating conditions. For example, tyre cornering stiffness varies with vertical load and road surface characteristics, and the height of the vehicle's centre of gravity depends on the payload config-

uration. In order to design a practical active roll control system, it is necessary to use a simplified vehicle model with some estimates of vehicle parameters and some simplifications of component response characteristics. However, the controlled system should remain stable even when the vehicle parameters vary within reasonable bounds from the nominal values. Although the linear quadratic regulator has guaranteed stability margins in the form of gain margin, gain reduction margin and phase margin, it is also necessary to verify that the stability of a controlled vehicle is robust in the presence of model uncertainties.

The following is a list of important vehicle parameters that were assumed to vary from the nominal values used in the linear vehicle model:

- The vehicle sprung mass and the sprung mass height were assumed to both vary by $\pm 15\%$, to represent uncertainty in payload configuration for a fully loaded vehicle.
- The average tyre cornering stiffnesses were assumed to vary between the nominal value and 0.65 of this value, to represent the effects of variations in tyre and road conditions.
- The front-to-rear balance in tyre cornering stiffness was assumed to vary by $\pm 15\%$ from the nominal balance, to account for changes in handling characteristics due to lateral load transfers during severe manoeuvres.
- Both suspension roll stiffnesses were varied between the nominal value and a value 15% lower, to account for the nonlinear response of air springs and dampers and geometric nonlinearities in the suspension system.
- An additional phase lag represented by a first-order filter with bandwidth as low as 2 Hz was introduced at each active anti-roll bar, to represent unforeseen actuator performance limitations.
- The vehicle speed was assumed to vary about the design set point by $\pm 10\%$. A

practical active roll control system would schedule controller gains according to vehicle speed.

The effect of vehicle parameter uncertainty on the closed loop stability of the torsionally flexible single unit vehicle model is shown in figure 11. The stability of the closed loop system for all combinations of nominal, maximum and minimum vehicle parameters is plotted. The nominal system poles are denoted by the symbol (\circ). The closed loop poles of the system remain in the open left half plane for all combinations of possible parameter variations, so the system is robustly stable in the presence of model uncertainty.

4.4.8 Effect on handling performance

The effect of active roll control on the handling performance of the torsionally flexible single unit vehicle model with nonlinear tyres (equation (1)) at 60 km/h is shown in figure 12.

First, consider the response of the vehicle without active roll control. At low levels of lateral acceleration, the vehicle understeers mildly. As lateral acceleration increases, the normalised load transfer builds up more quickly at the drive axle than at the steer axle. There is a reduction in the cornering stiffness of the rear relative to the front and the handling changes from neutral steer to oversteer by 0.3 g. The drive axle lifts off at 0.38 g, by which point the yaw stability of the vehicle is significantly reduced. This effect is more pronounced for a more torsionally flexible vehicle frame.

Despite the presence of torsional compliance in the vehicle frame, the active roll control system balances the build up of normalised load transfer evenly between the steer and drive axles. The understeer gradient builds up as lateral acceleration increases and the vehicle remains understeering throughout. The active roll control system appreciably increases the level of yaw stability at high levels of lateral acceleration. The handling performance of the torsionally flexible vehicle equipped with an active roll control system is similar to that of the torsionally rigid active vehicle [19].

5 Conclusions

1. Active roll control is a problem of optimal disturbance rejection, which is an extension of the standard LQR problem. It was shown that, in order to maximise roll stability, the steering disturbance must either be measured or estimated and incorporated into the feedback law.
2. A practical partial-state feedback controller, using measurements of suspension roll angles, body roll rate, yaw rate and steering input, can be designed using the linear quadratic Gaussian-loop transfer recovery technique.
3. Simulations showed that a system of active anti-roll bars incorporating moderately priced, low bandwidth hydraulic actuators and servo-valves and relatively simple instrumentation can improve steady-state roll stability of a torsionally flexible single unit vehicle by 26%. Improvements in severe transient manoeuvres were even greater: approximately 38% for a step steering input and 46% for a double lane change manoeuvre. These figures represent a significant increase in vehicle safety.
4. By distributing the total normalised load transfer between the steer and drive axles in a balanced fashion, active roll control tends to increase understeer for a typical single unit vehicle.
5. The performance of the control strategies described here will be validated using the experimental vehicle that is currently being developed at the University of Cambridge.

Acknowledgements

The authors wish to acknowledge the financial support of the Cambridge Vehicle Dynamics Consortium and the Engineering and Physical Sciences Research Council. At the time of writing, the Cambridge Vehicle Dynamics Consortium consisted of the Cambridge and Cranfield Universities together with the following industrial partners from the European heavy vehicle industry: Tinsley Bridge Ltd, ArvinMeritor, Koni BV, Qinetiq, Pirelli, Shell UK Ltd, Volvo Global Trucks, General Trailers, Firestone Industrial Products, Mektronika Systems and Fluid Power Design. Dr Sampson would like to thank the Cambridge Australia Trust and the Committee of Vice-Chancellors and Principals of the Universities of the United Kingdom for their support.

A Equations of motion

The equations of motion for the linear torsionally flexible single unit vehicle (figure 1) are

$$m_{s,f}h_f\ddot{\phi}_f + m_{s,r}h_r\ddot{\phi}_r = -mU(\dot{\beta} + \dot{\psi}) + Y_\beta\beta + Y_{\dot{\psi}}\dot{\psi} + Y_\delta\delta, \quad (\text{A1})$$

$$-I_{x'z',f}\ddot{\phi}_f - I_{x'z',r}\ddot{\phi}_r + I_{z'z'}\ddot{\psi} = N_\beta\beta + N_{\dot{\psi}}\dot{\psi} + N_\delta\delta, \quad (\text{A2})$$

$$\begin{aligned} I_{x'x',f}\ddot{\phi}_f - I_{x'z',f}\ddot{\psi} &= m_{s,f}gh_f\phi_f - m_{s,f}Uh_f(\dot{\beta} + \dot{\psi}) \\ &\quad - k_f(\phi_f - \phi_{t,f}) - l_f(\dot{\phi}_f - \dot{\phi}_{t,f}) \\ &\quad - k_b(\phi_f - \phi_r) - l_b(\dot{\phi}_f - \dot{\phi}_r) \\ &\quad - F_bh_b + u_f, \end{aligned} \quad (\text{A3})$$

$$\begin{aligned} I_{x'x',r}\ddot{\phi}_r - I_{x'z',r}\ddot{\psi} &= m_{s,r}gh_r\phi_r - m_{s,r}Uh_r(\dot{\beta} + \dot{\psi}) \\ &\quad - k_r(\phi_r - \phi_{t,r}) - l_r(\dot{\phi}_r - \dot{\phi}_{t,r}) \\ &\quad + k_b(\phi_f - \phi_r) + l_b(\dot{\phi}_f - \dot{\phi}_r) \\ &\quad + F_bh_b + u_r, \end{aligned} \quad (\text{A4})$$

$$\begin{aligned} -r(Y_{\beta,f}\beta + Y_{\dot{\psi},f}\dot{\psi} + Y_{\delta,f}\delta) &= m_{u,f}U(h_{u,f} - r)(\dot{\beta} + \dot{\psi}) + k_{t,f}\phi_{t,f} \\ &\quad - m_{u,f}gh_{u,f}\phi_{t,f} - k_f(\phi_f - \phi_{t,f}) \\ &\quad - l_f(\dot{\phi}_f - \dot{\phi}_{t,f}) + u_f, \end{aligned} \quad (\text{A5})$$

$$\begin{aligned} -r(Y_{\beta,r}\beta + Y_{\dot{\psi},r}\dot{\psi}) &= m_{u,r}V(h_{u,r} - r)(\dot{\beta} + \dot{\psi}) + k_{t,r}\phi_{t,r} \\ &\quad - m_{u,r}gh_{u,r}\phi_{t,r} - k_r(\phi_r - \phi_{t,r}) \\ &\quad - l_r(\dot{\phi}_r - \dot{\phi}_{t,r}) + u_r. \end{aligned} \quad (\text{A6})$$

Equation (A1) is a lateral force balance for the entire vehicle. Equation (A2) is a yaw moment balance for the entire vehicle. Equations (A3) and (A4) describe the balance of roll moments on the sprung mass. Equations (A5) and (A6) describe the roll motions of the front and rear unsprung masses respectively.

Body inertia

Vehicle unit	m_s	I_{xx}	I_{zz}	I_{xz}
Tractor	4819	2411	11383	1390
Units	kg	kg.m ²	kg.m ²	kg.m ²

Axle geometry

Vehicle unit	Axle	a^*	h_u	d	Δd
Tractor	steer	0.000	0.530	2.000	—
Tractor	drive	3.700	0.530	1.800	0.429
Units		m	m	m	m

Axle inertia

Vehicle unit	Axle	m_u	I_{xx}	I_{zz}	I_{xz}
Tractor	steer	706	440	440	0
Tractor	drive	1000	563	563	0
Units		kg	kg.m ²	kg.m ²	kg.m ²

Additional lumped mass inertia

Vehicle unit	m_s	I_{xx}	I_{zz}	I_{xz}
Tractor	8828	792	792	0
Units	kg	kg.m ²	kg.m ²	kg.m ²

Frame and coupling properties

Vehicle unit	k_b
Tractor	629
Units	kN.m/rad

Suspension properties

Vehicle unit	Axle	k	L
Tractor	steer	380	4.05
Tractor	drive	684	6.68
Units		kN.m/rad	kN.m.s/rad

Tyre properties

Vehicle unit	Axle	c_1	c_2	k_t^{\ddagger}	M^{\S}
Tractor	steer	10.34	90.9	2060	6053
Tractor	drive	10.34	90.9	3337	9300
Units		rad ⁻¹	MN ⁻¹ .rad ⁻¹	kN.m/rad	kg

[‡]Total tyre roll stiffness for the axle: steer axle is fitted with single tyres, drive axle is fitted with dual tyres.

[§]Axle weight including the additional lumped mass.

C Nomenclature

A, B, C, D	state-space matrices
a'	longitudinal distance to axle, measured forwards from centre of total mass
a^*	longitudinal distance to axle, measured backwards from front axle (trucks and tractors) or from front articulation point (dollies and semi-trailers)
a_y	lateral acceleration
b	longitudinal distance to articulation point, measured forwards from centre of sprung mass
b'	longitudinal distance to articulation point, measured forwards from centre of total mass
b^*	longitudinal distance to rear articulation point, measured backwards from front axle (tractors) or from front articulation point (dollies and semi-trailers)
c_1, c_2	tyre cornering stiffness coefficients, in $\frac{F_y}{\alpha} = c_1 \times F_z + c_2 \times F_z^2$
c_α	tyre cornering stiffness, measured at rated vertical tyre load
d	track width
Δd	tyre spread (for axles with twin tyres)
F_b	lateral shear force in vehicle frame
F_y	lateral tyre force
F_z	vertical tyre force
g	acceleration due to gravity
h	height centre of sprung mass, measured upwards from roll centre
h_b	height of frame twist axis, measured upwards from ground
h_{cm}	height of total centre of mass, measured upwards from ground
h_s	height of centre of sprung mass, measured upwards from ground
h_u	height of centre of unsprung mass, measured upwards from ground
I_{xx}	roll moment of inertia of sprung mass, measured about sprung centre of mass
$I_{x'x'}$	roll moment of inertia of sprung mass, measured about origin of (x', y', z') coordinate system
I_{xz}	yaw-roll product of inertia of sprung mass, measured about sprung centre of mass
$I_{x'z'}$	yaw-roll product of inertia of sprung mass, measured about origin of (x', y', z') coordinate system
I_{zz}	yaw moment of inertia of sprung mass, measured about sprung centre of mass

$I_{z'z'}$	yaw moment of inertia of total mass, measured about origin of (x', y', z') coordinate system
J	quadratic performance index
k	suspension roll stiffness
k_b	vehicle frame torsional stiffness
k_t	tyre roll stiffness
l	suspension roll damping rate
l_b	vehicle frame torsional damping rate
m	total mass
m_s	sprung mass
m_u	unsprung mass
N_β	$\frac{\partial M_z}{\partial \beta} = \sum_j a'_j c_{\alpha,j}$ partial derivative of net tyre yaw moment with respect to sideslip angle
N_δ	$\frac{\partial M_z}{\partial \delta} = -a'_1 c_{\alpha,1}$ partial derivative of net tyre yaw moment with respect to steer angle
$N_{\dot{\psi}}$	$\frac{\partial M_z}{\partial \dot{\psi}} = \sum_j \frac{a_j'^2 c_{\alpha,j}}{U}$ partial derivative of net tyre yaw moment with respect to yaw rate
Q	performance output weighting matrix
R	control input weighting matrix
r	height of roll axis, measured upwards from ground
U	forward speed
u	active roll torque
V	process noise weighting matrix
W	measurement noise weighting matrix
x	state vector
x'	longitudinal distance, measured forwards from centre of total mass
x_D	disturbance state vector
y	measurement output
y'	lateral distance, measured to the right from vehicle unit centreline
Y_β	$\frac{\partial F_y}{\partial \beta} = \sum_j c_{\alpha,j}$ partial derivative of net tyre lateral force with respect to sideslip angle
Y_δ	$\frac{\partial F_y}{\partial \delta} = -c_{\alpha,1}$ partial derivative of net tyre lateral force with respect to steer angle

$Y_{\dot{\psi}}$	$\frac{\partial F_y}{\partial \dot{\psi}} = \sum_j \frac{a'_j c_{\alpha,j}}{U}$	partial derivative of net tyre lateral force with respect to yaw rate
z		performance output
z'		vertical distance, measured downwards from roll axis
α		tyre slip angle
β		sideslip angle
γ		frame twist angle
δ		steer angle
ϕ		absolute roll angle of sprung mass
ϕ_t		absolute roll angle of unsprung mass
$\dot{\psi}$		yaw rate

Additional subscripts

f	front
i	i th vehicle unit, or i th vehicle coupling, counted from front
j	j th axle, counted from front
r	rear

References

- [1] Abe, M. A study on effects of roll moment distribution control in active suspension on improvement of limit performance of vehicle handling. *International Journal of Vehicle Design*, 15(3–5):326–336, 1994.
- [2] Bryson, A. E. and Ho, Y. C. *Applied Optimal Control*. Blaisdell, Waltham, MA, USA, second edition, 1975.
- [3] Doyle, J. C. and Stein, G. Robustness with observers. *IEEE Transactions on Automatic Control*, 24(2):607–611, 1979.
- [4] Dunwoody, A. B. and Froese, S. Active roll control of a semi-trailer. *SAE Transactions*, 102(933045):999–1004, 1993.
- [5] Fancher, P. S., Ervin, R. D., Winkler, C. B., and Gillespie, T. D. A factbook of the mechanical properties of the components for single-unit and articulated heavy trucks. Technical Report UMTRI-86-12, University of Michigan Transportation Research Institute, Ann Arbor, MI, USA, 1986.
- [6] Gillespie, T. D. *Fundamentals of Vehicle Dynamics*. SAE, Warrendale, PA, USA, 1992.
- [7] Hwang, S.-M. and Park, Y. Active roll moment distribution based on predictive control. *International Journal of Vehicle Design*, 16(1):15–28, 1995.
- [8] Kalman, R. When is a linear control system optimal? *ASME Transactions, Journal of Basic Engineering*, 86:51–60, 1964.
- [9] Kusahara, Y., Li, X., Hata, N., and Watanabe, Y. Feasibility study of active roll stabilizer for reducing roll angle of an experimental medium-duty truck. In *Proc. 2nd International Symposium on Advanced Vehicle Control*, pages 343–348, Tsukuba, Japan, 1994.

- [10] Lin, C.-F. *Modern Navigation, Guidance, and Control Processing*. Prentice Hall, Upper Saddle River, NJ, USA, 1991.
- [11] Lin, C.-F. *Advanced Control Systems Design*. Prentice Hall, Upper Saddle River, NJ, USA, 1994.
- [12] Lin, R. C. *An Investigation of Active Roll Control for Heavy Vehicle Suspensions*. Ph.D. thesis, University of Cambridge, Cambridge, UK, 1994.
- [13] Lin, R. C., Cebon, D., and Cole, D. J. Investigation of active roll control of heavy road vehicles. In *Proc. 14th IAVSD Symposium on the Dynamics of Vehicles on Roads and Tracks*, pages 308–321, Chengdu, China, 1993.
- [14] Lin, R. C., Cebon, D., and Cole, D. J. Active roll control of articulated vehicles. *Vehicle System Dynamics*, 26(1):17–43, 1996.
- [15] Lin, R. C., Cebon, D., and Cole, D. J. Optimal roll control of a single-unit lorry. *Proc. IMechE, Journal of Automobile Engineering*, 210(1):44–55, 1996.
- [16] McKevitt, P. G. *Design of Roll Control Systems for Heavy Vehicles*. M.Phil. thesis, University of Cambridge, Cambridge, UK, 1999.
- [17] Pflug, H. C., von Glasner, E.-Ch., and Povel, R. Improvement of commercial vehicles' handling and stability by smart chassis systems. In Pauwelussen, J. P. and Pacejka, H. B., editors, *Smart Vehicles*, pages 318–338. Swets and Zeitlinger, Lisse, The Netherlands, 1995.
- [18] Safonov, M. G. and Athans, M. Gain and phase margin for multiloop LQG regulators. *IEEE Transactions on Automatic Control*, 22(2):173–179, 1977.
- [19] Sampson, D. J. M. *Active Roll Control of Articulated Heavy Vehicles*. Ph.D. thesis, University of Cambridge, Cambridge, UK, 2000.
- [20] Sampson, D. J. M. and Cebon, D. Achievable roll stability of heavy road vehicles. Submitted to *Proc. IMechE, Journal of Automobile Engineering*, 2001.

- [21] Segel, L. Theoretical prediction and experimental substantiation of the response of an automobile to steering control. *Proc. IMechE, Automotive Division*, pages 310–330, 1956–57.
- [22] Shannan, J. E. and van der Ploeg, M. J. A vehicle handling model with active suspensions. *Journal of Mechanisms, Transmissions and Automation in Design*, 111:375–381, 1989.
- [23] Skogestad, S. and Postlethwaite, I. *Multivariable Feedback Control – Analysis and Design*. John Wiley & Sons, Chichester, UK, 1996.
- [24] Williams, D. E. and Haddad, W. M. Nonlinear control of roll moment distribution to influence vehicle yaw characteristics. *IEEE Transactions on Control Systems Technology*, 3(1):110–116, 1995.
- [25] Winkler, C. B., Blower, D., Ervin, R. D., and Chalasani, R. M. *Rollover of Heavy Commercial Vehicles*. SAE, Warrendale, PA, USA, 2000.

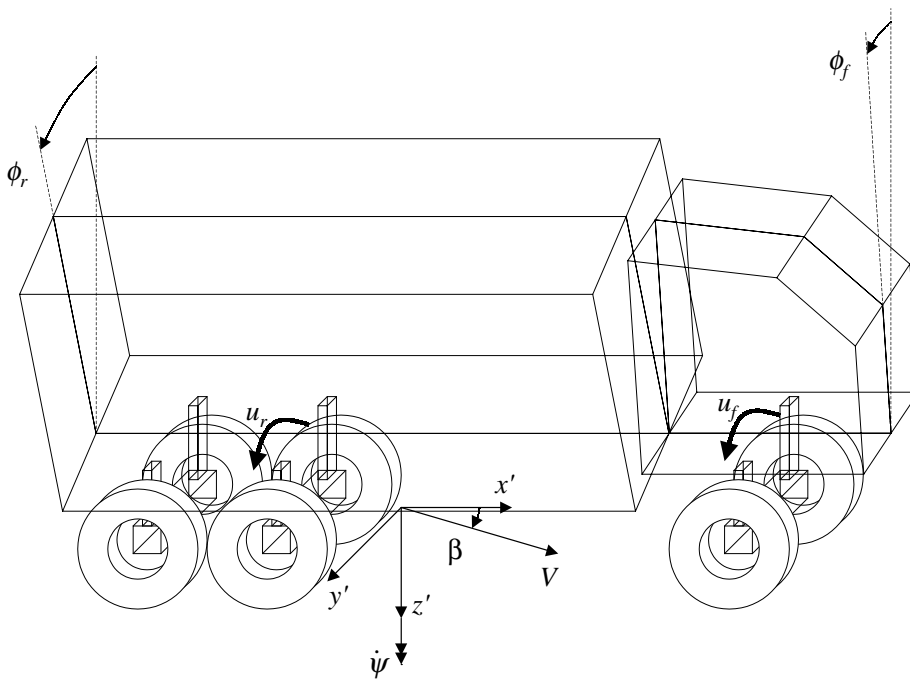
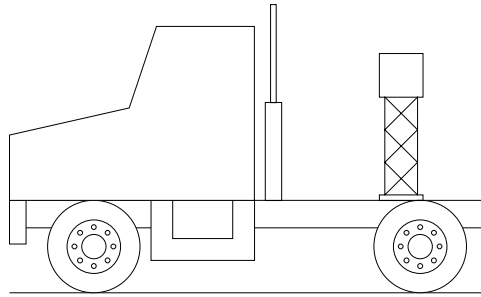
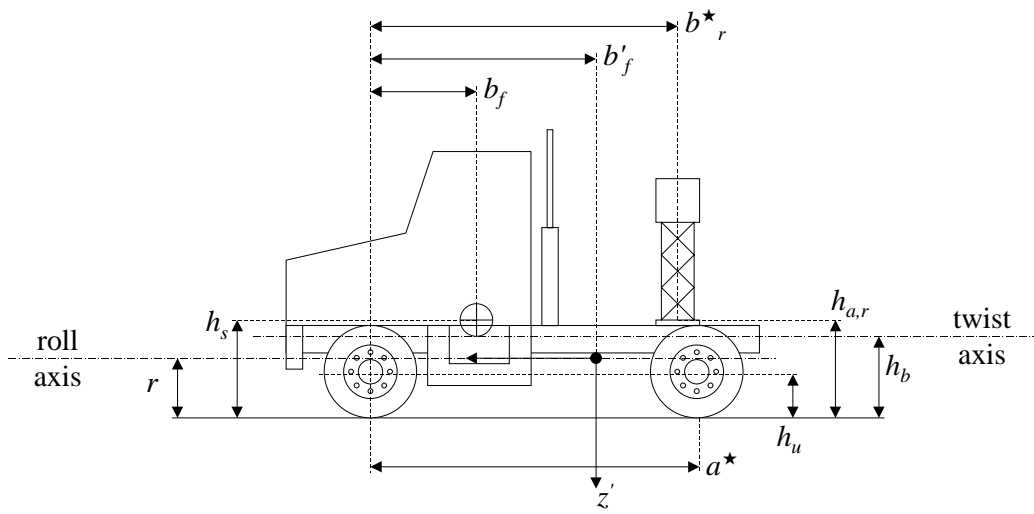


Figure 1: Single unit vehicle with flexible frame (ϕ_f, ϕ_r measured from vertical).



(a) Schematic.



(b) Dimensions.

Figure 2: Single unit vehicle with lumped mass.

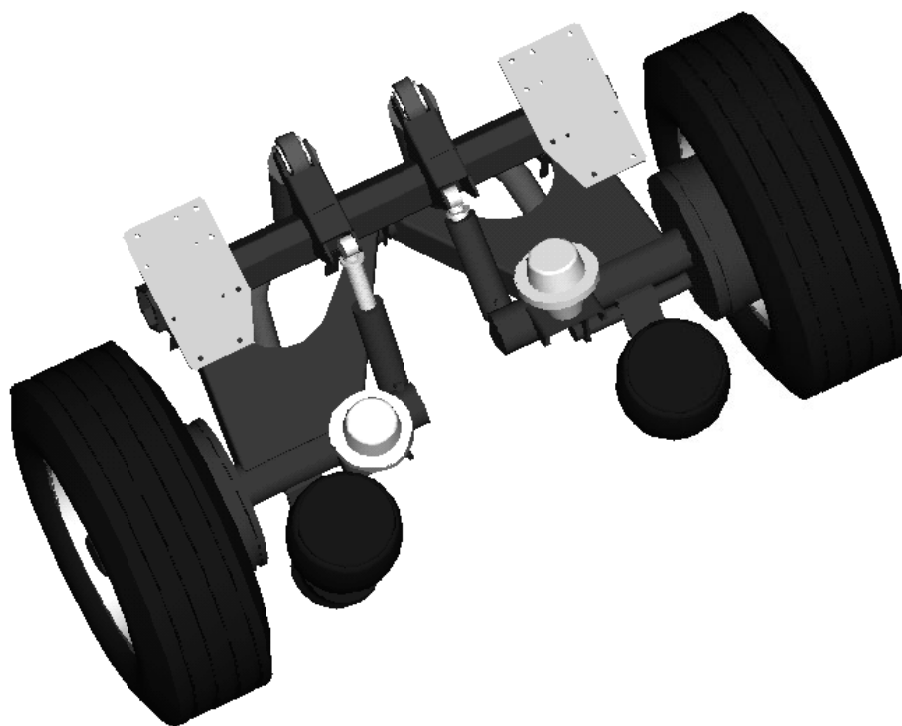
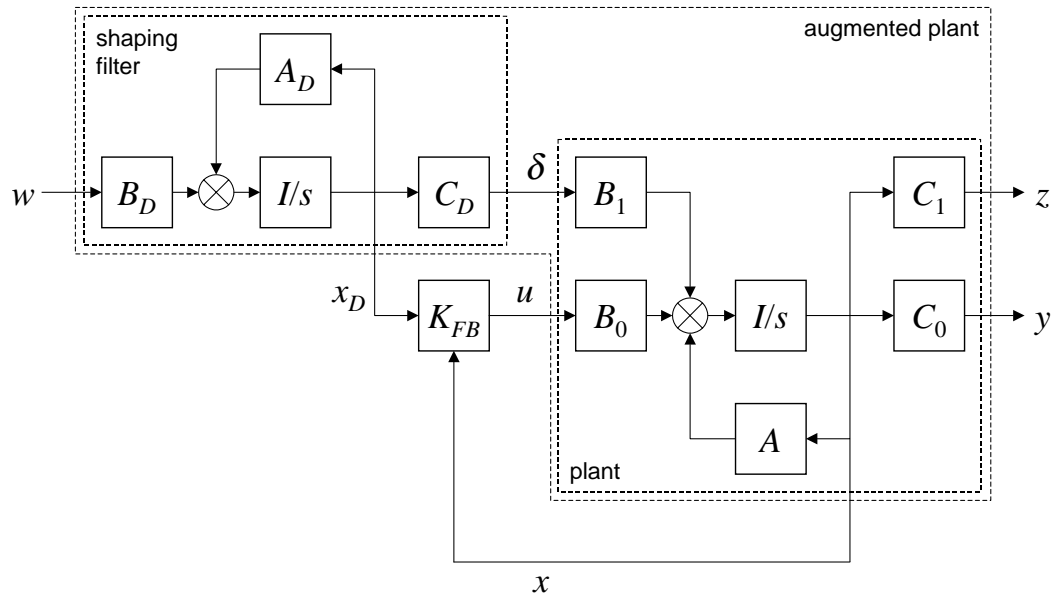
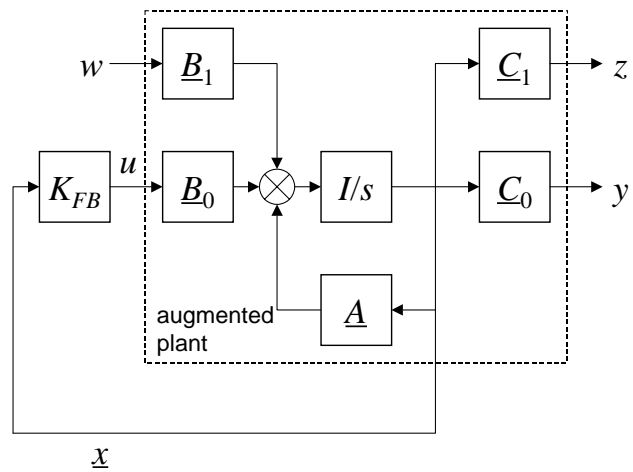


Figure 3: Active anti-roll bar general arrangement [16].

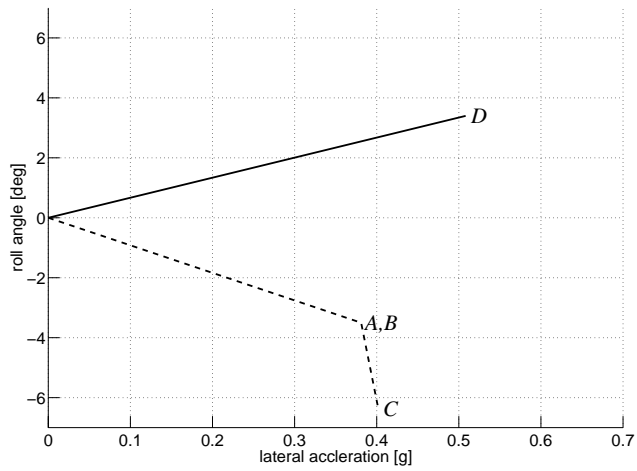


(a) Detailed model showing the shaping filter and the plant.

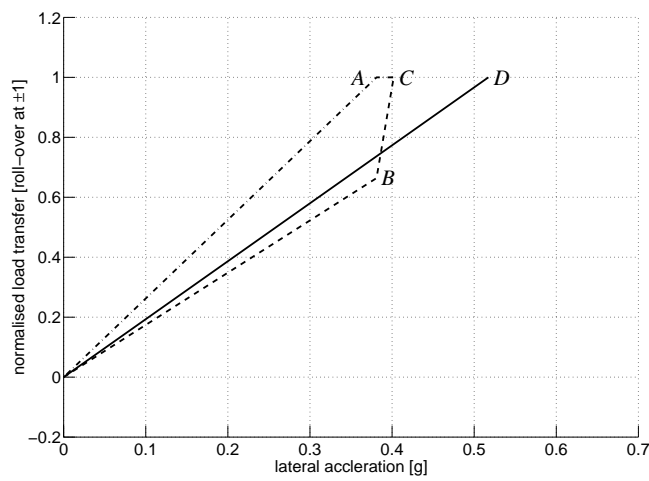


(b) Simplified model showing the augmented plant.

Figure 4: Optimal disturbance rejection.

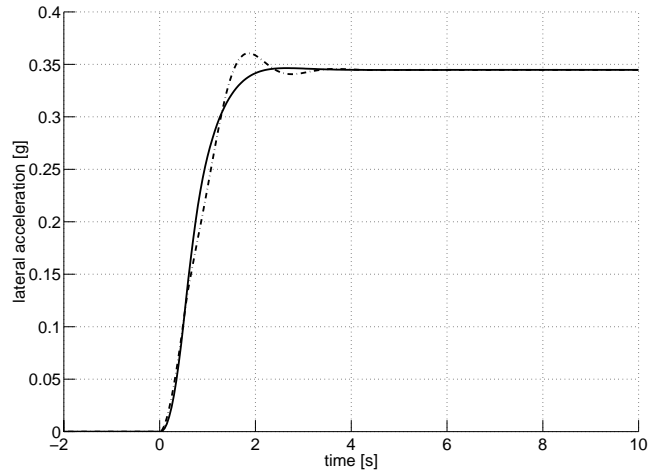


(a) Suspension roll angles. Active roll control: *steer axle* (—); passive suspension: *steer axle* (- - -).

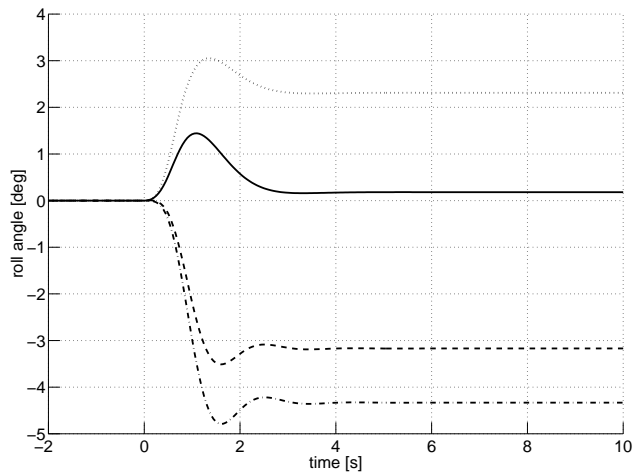


(b) Normalised load transfers. Active roll control: *steer axle and drive axle* (—); passive suspension: *steer axle* (- - -), *drive axle* (· - · - ·).

Figure 5: Response of the linear, torsionally flexible single unit vehicle model with a full-state feedback controller to a steady-state steering input.

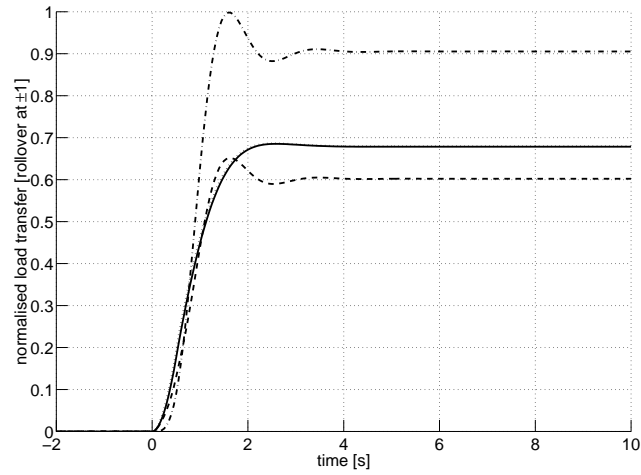


(a) Lateral acceleration. Active roll control (—), passive suspension (· - · - ·).

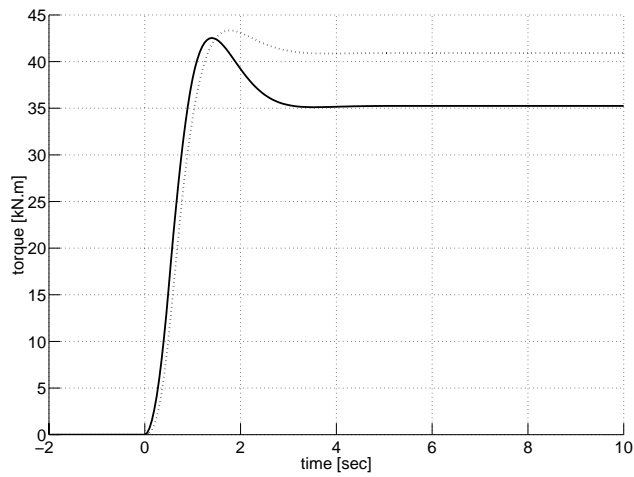


(b) Suspension roll angles. Active roll control: *steer axle* (· · · · ·), *drive axle* (—); passive suspension: *steer axle* (- - -), *drive axle* (· - · - ·).

Figure 6: Response of the linear, torsionally flexible single unit vehicle model with a full-state feedback controller to a step steering input.

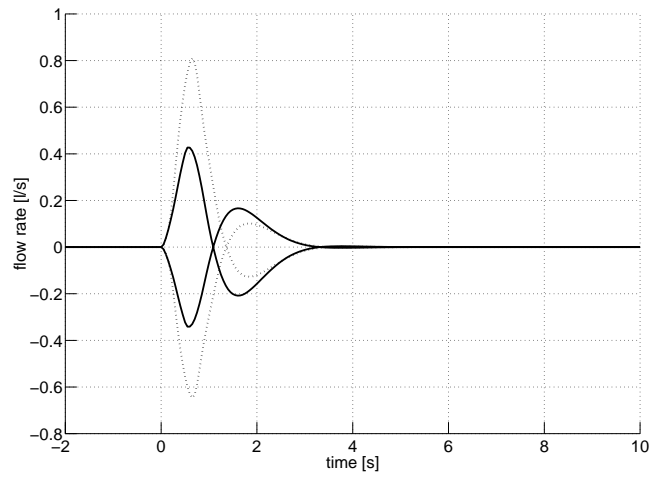


(c) Normalised load transfers. Active roll control: *steer axle* (·····), *drive axle* (—); passive suspension: *steer axle* (---), *drive axle* (·-·-·).



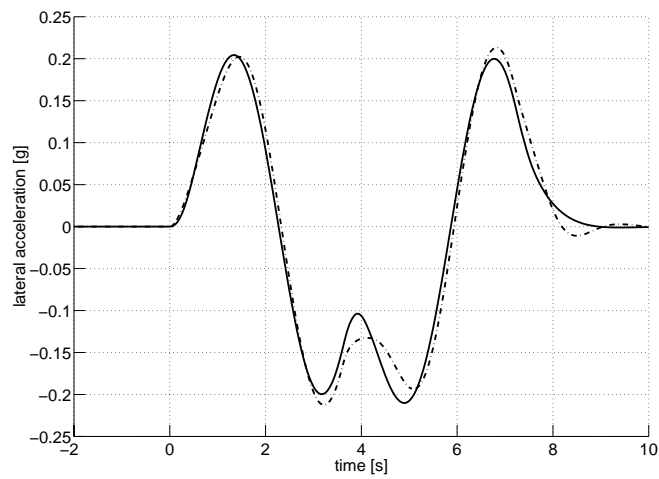
(d) Active anti-roll bar moments. Active roll control: *steer axle* (·····), *drive axle* (—).

Figure 6: Continued.



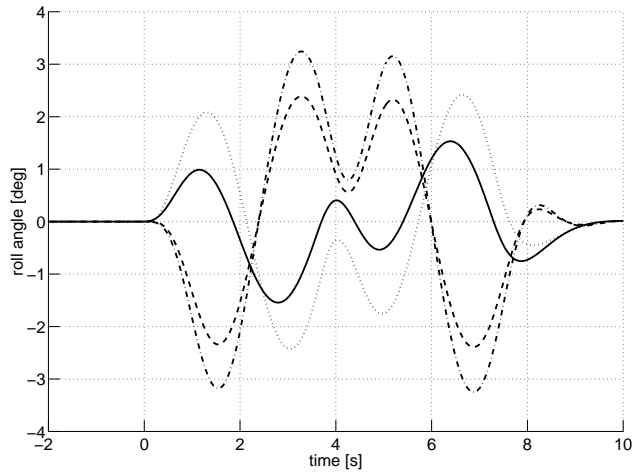
(e) Servo-valve flow rates. Active roll control: *steer axle* (·····), *drive axle* (—).

Figure 6: Continued.

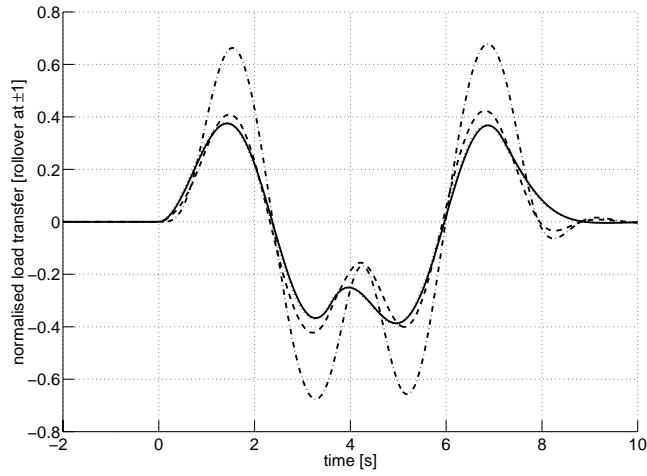


(a) Lateral acceleration. Active roll control (—), passive suspension (· - · - ·).

Figure 7: Response of the linear, torsionally flexible single unit vehicle model with a full-state feedback controller to a double lane change steering input.

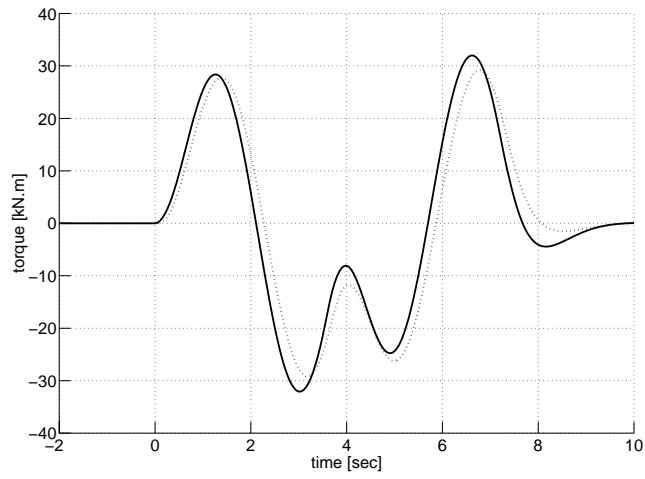


(b) Suspension roll angles. Active roll control: *steer axle* (·····), *drive axle* (—); passive suspension: *steer axle* (---), *drive axle* (·-·-·).

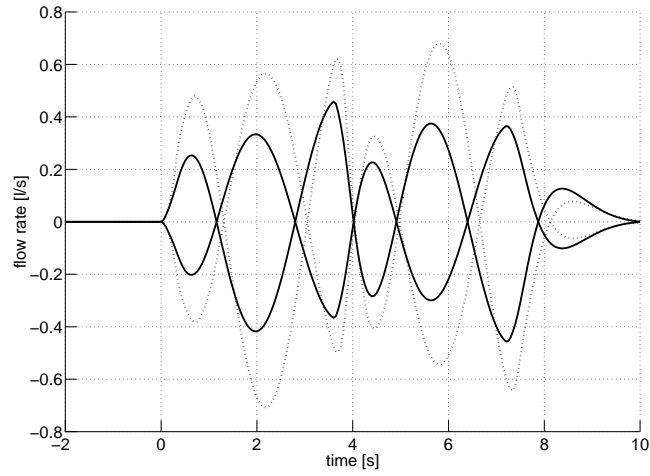


(c) Normalised load transfers. Active roll control: *steer axle* (·····), *drive axle* (—); passive suspension: *steer axle* (---), *drive axle* (·-·-·).

Figure 7: Continued.

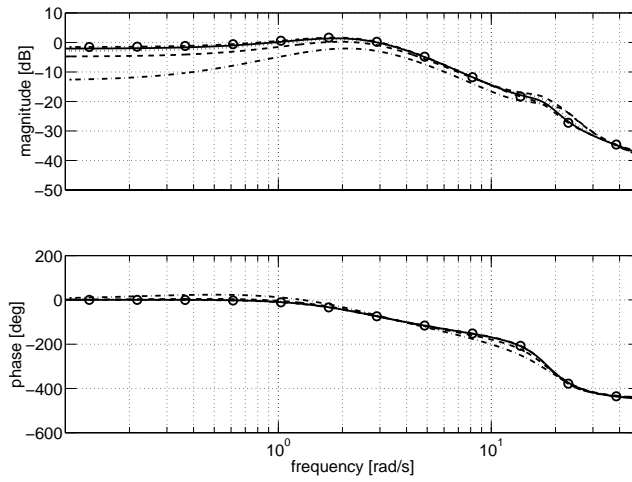


(d) Active anti-roll bar moments. Active roll control: *steer axle* (·····), *drive axle* (—).

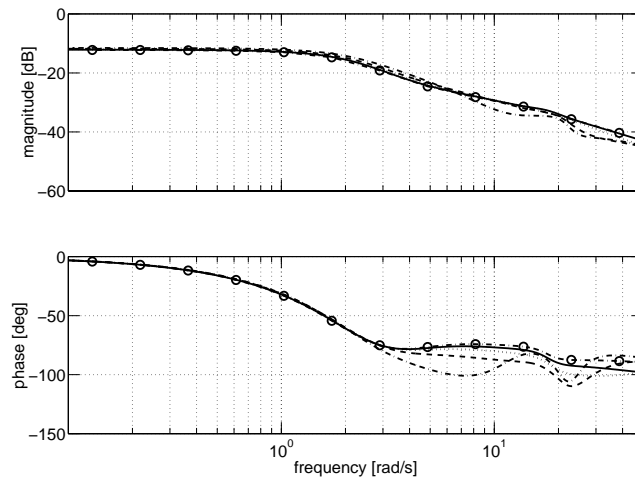


(e) Servo-valve flow rates. Active roll control: *steer axle* (·····), *drive axle* (—).

Figure 7: Continued.

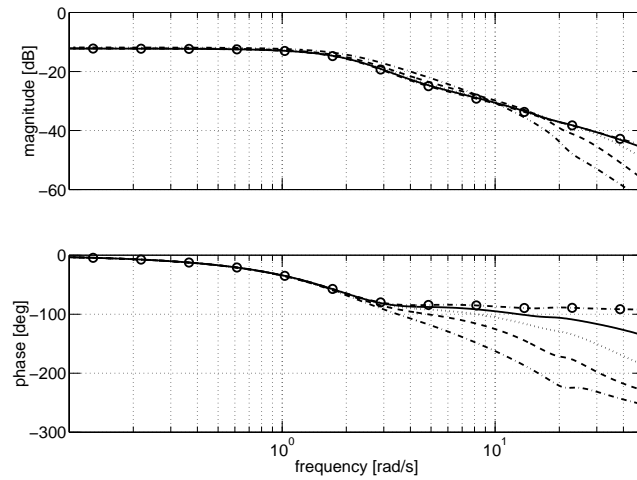


(a) From steering input [deg] to steer axle suspension roll angle [deg]. Partial-state feedback control: $V = 0.001$ (—), 0.01 (·····), 0.1 (---), 1 (-·-·-·); full-state feedback control: (·-○-·-·).



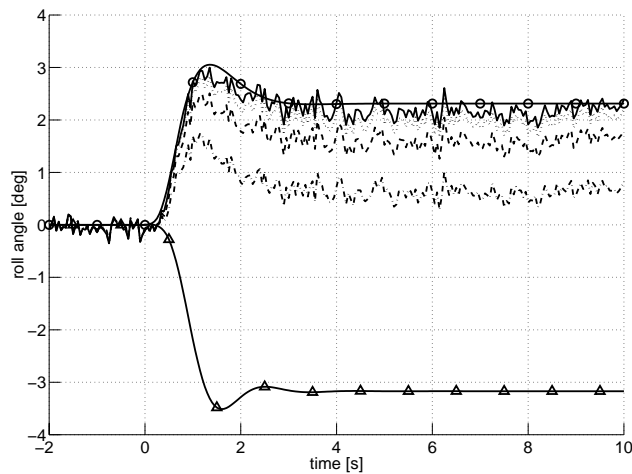
(b) From steering input [deg] to normalised steer axle load transfer [roll-over at ± 1]. Partial-state feedback control: $V = 0.001$ (—), 0.01 (·····), 0.1 (---), 1 (-·-·-·); full-state feedback control: (·-○-·-·).

Figure 8: Variation with Kalman filter design weights of the frequency response of the linear, torsionally flexible single unit vehicle model with a partial-state feedback controller.



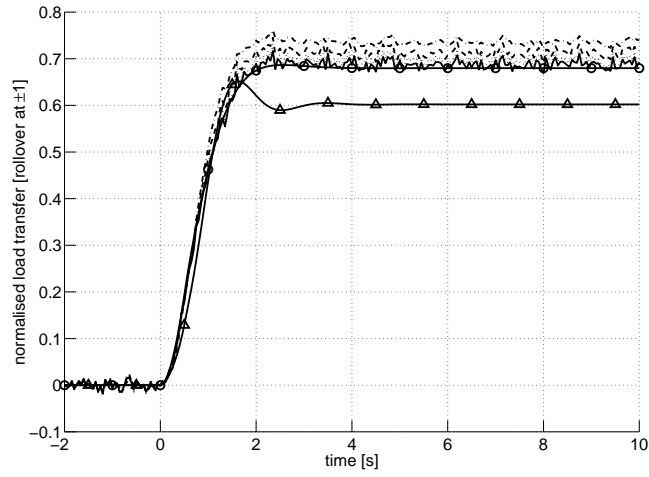
(c) From steering [deg] to normalised drive axle load transfer. Partial-state feedback control: $V = 0.001$ (—), 0.01 (·····), 0.1 (---), 1 (·-·-·); full-state feedback control: (·-○-·).

Figure 8: Continued.

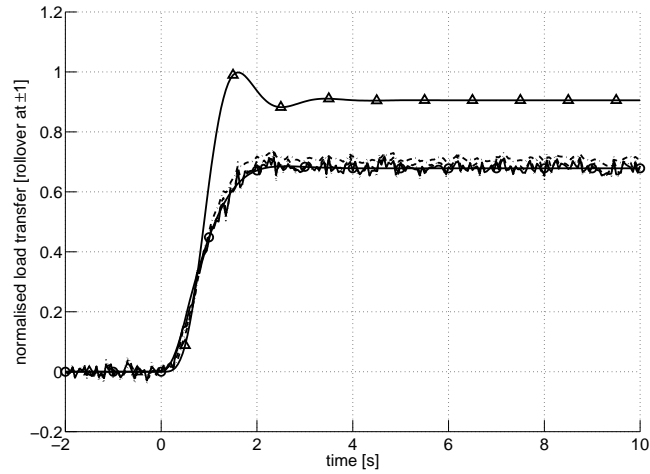


(a) Steer axle suspension roll angle [deg]. Partial-state feedback control: $V = 0.001$ (—), 0.01 (·····), 0.1 (---), 1 (·-·-·); full-state feedback control: (·-○-·); passive control: (-△-).

Figure 9: Variation with Kalman filter design weights of the response of the linear, torsionally flexible single unit vehicle model with a partial-state feedback controller.

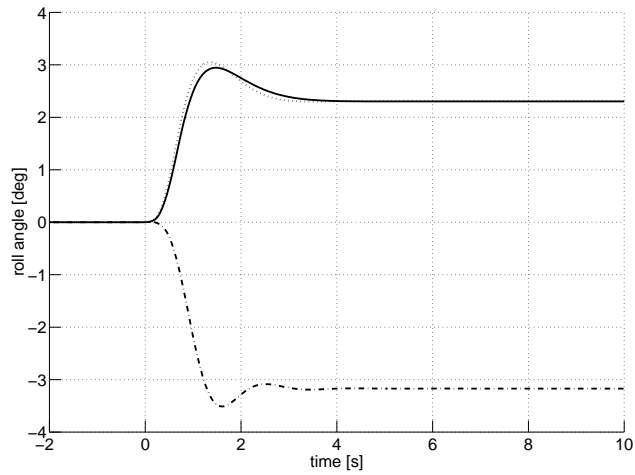


(b) Normalised steer axle load transfer. Partial-state feedback control: $V = 0.001$ (—), 0.01 (·····), 0.1 (---), 1 (·-·-·); full-state feedback control: (·-○-·); passive control: (-△-).

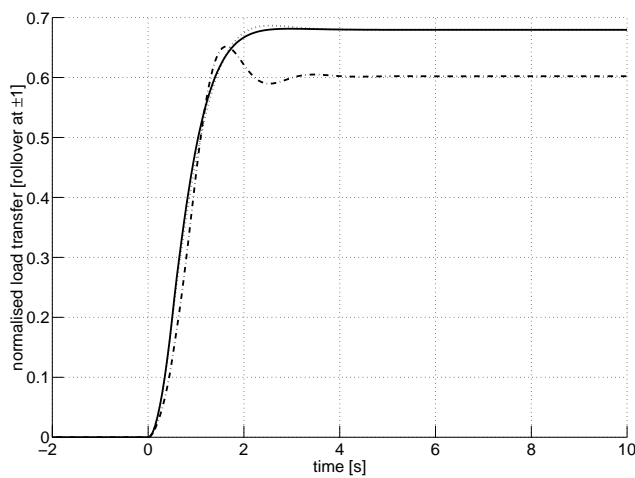


(c) Normalised drive axle load transfer. Partial-state feedback control: $V = 0.001$ (—), 0.01 (·····), 0.1 (---), 1 (·-·-·); full-state feedback control: (·-○-·); passive control: (-△-).

Figure 9: Continued.

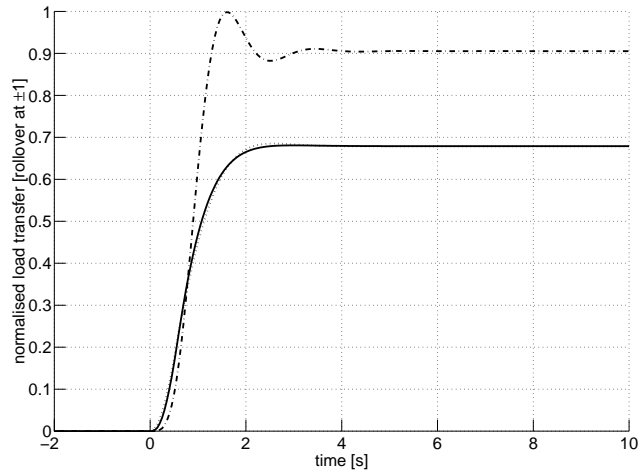


(a) Steer axle suspension roll angle. Full-state feedback control: ∞ bandwidth (·····), 0.5 Hz bandwidth (—); passive control: (· - · - ·).

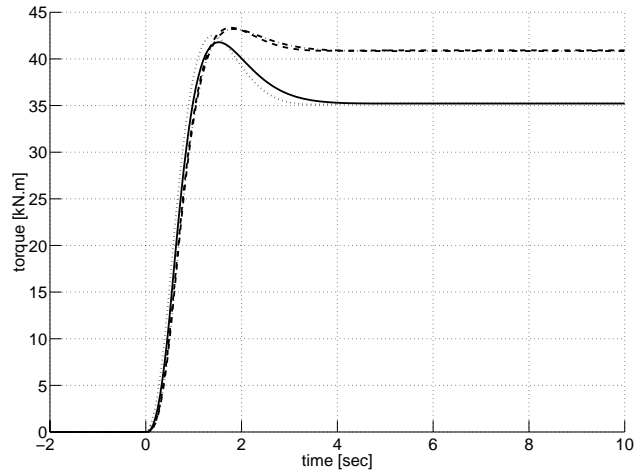


(b) Normalised steer axle load transfer. Full-state feedback control: ∞ bandwidth (·····), 0.5 Hz bandwidth (—); passive control: (· - · - ·).

Figure 10: Effect of limited actuator bandwidth on the response of the linear, torsionally flexible single unit vehicle model with a full-state feedback controller to a step steering input.

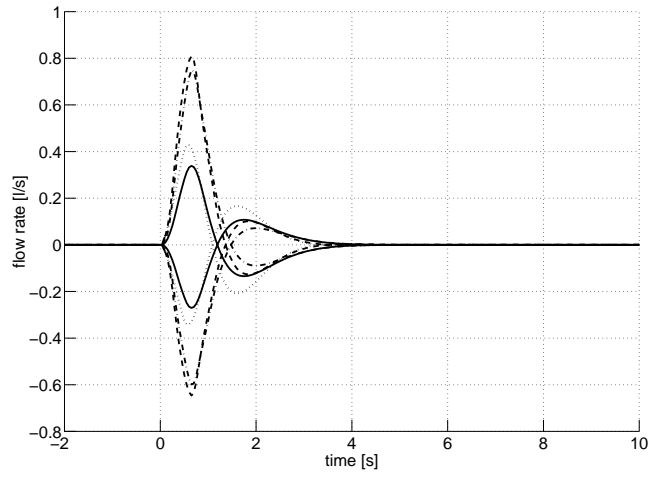


(c) Normalised drive axle load transfer. Full-state feedback control: ∞ bandwidth (·····), 0.5 Hz bandwidth (—); passive control: (·-·-·).



(d) Active anti-roll bar moments. ∞ bandwidth: *steer axle* (·····), *drive axle* (---); 0.5 Hz bandwidth: *steer axle* (—), *drive axle* (·-·-·).

Figure 10: Continued.



(e) Servo-valve flow rates. ∞ bandwidth: *steer axle* ($\cdots\cdots$), *drive axle* ($----$); 0.5 Hz bandwidth: *steer axle* ($—$), *drive axle* ($- \cdot - \cdot -$).

Figure 10: Continued.

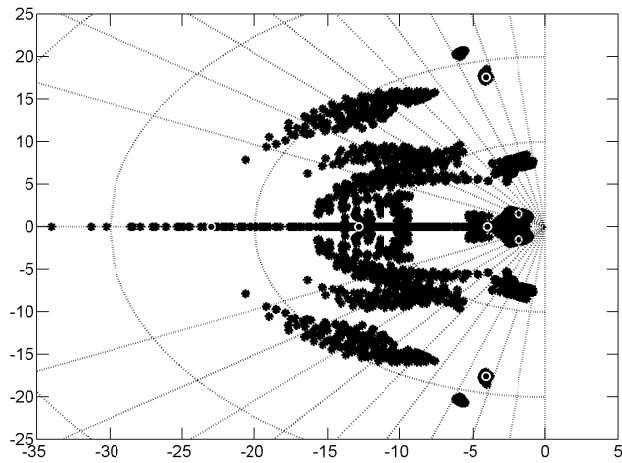
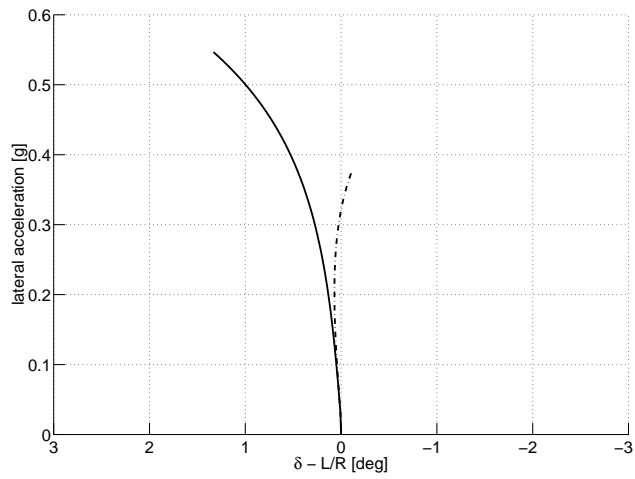


Figure 11: Variation with selected vehicle parameters of the closed-loop poles of the torsionally flexible single unit vehicle with a full-state feedback controller.



Active roll control (—), passive suspension (· - · - ·).

Figure 12: Handling diagram for the torsionally flexible single unit vehicle with a full-state feedback controller.